

A COMPACT MULTIMODE BANDPASS FILTER WITH EXTENDED STOPBAND BANDWIDTH

K. Ma^{*}, S. Mou, K. Wang, and K. S. Yeo

School of Electrical and Electronic Engineering, Nanyang Technological University, Singapore

Abstract—A compact multimode bandpass filter with low insertion loss, high stopband rejection and wide stopband bandwidth is introduced by using cascaded multimode resonators and compact loading cells in combination. The measured minimum insertion loss is of 1.7 dB including the connector loss in the input and output ports in the passband of 5.7 ~ 8 GHz. Through the use of cascaded multimode resonators, steep skirt selectivity and wide stopband up to 18 GHz can be achieved. When incorporated with the lowpass loading cells, which have elliptical low-pass response by using the source-load coupling, the stopband of the proposed filter can be further extended up to 40 GHz, with only negligible influence on the passband performance.

1. INTRODUCTION

Microwave filters with high-performance and compact size are highly demanded in wireless communication systems [1–8]. Resonators, as fundamental elements in a filter [1–16], usually determine the size of the filter. Reducing resonator size is an effective approach to miniaturize the filter size. Normally, two approaches are used to reduce the resonator size. One approach is to modify the physical structures [8–10]. Another approach is to modify the traditional resonator to generate additional modes, which make the resonator to behave as a multimode resonator. Thus one physical resonator can be treated as multiple electrical resonators [11–18]. Although the multimode filters have advantages such as relative low insertion loss and compact size, there is a challenge to build the high order multimode filter due to the complexity of the coupling among the degenerated modes in the single multimode resonator. This is why

Received 22 April 2012, Accepted 13 June 2012, Scheduled 19 June 2012

* Corresponding author: Kaixue Ma (kxma@ntu.edu.sg).



Figure 1. The proposed dual-mode filter and its network model.

there are a lot of literatures describing the single multimode resonator, but a few literatures concentrating on multiple multimode resonators or filters [1–5]. Because the multiple degenerate modes and their parasitic resonances or modes, operate close to the fundamental mode, it is also a challenge to build the multimode resonator filter with a wide stopband [11–18]. The reported stopband bandwidth is too narrow to reject beyond the third parasitic spurious.

In this paper, an effective approach is adopted in high order multimode filter designs. The proposed approach helps to achieve the multimode operation with wide passband and ultra-wide stopband simultaneously. As shown in Figure 1, a single multimode resonator is extended to be high order multimode resonators. While keeping the good performance, the multimode resonators can be further optimized to have a much compact size. In addition, a loading cell (LC1 and LC2 in Figure 1) with elliptical low-pass response is introduced to extend the stopband bandwidth for the higher order multimode resonator filter. By doing so, a high order multimode filter with good merits of the passband and rolloff performances as well as an ultra-wide stopband can be achieved. The proposed approach is demonstrated by a multimode filter design with center frequency f_c of 7 GHz. Generally, based on the dedicated idea, the proposed multimode filter obtains a low insertion loss of 1.7 dB including the loss of the input/output port connectors, and an ultra-wide stopband up to $5.6f_c$.

2. CHARACTERISTICS OF MM RESONATOR

The MM resonator can be analyzed by using its equivalent circuits. As shown in Figure 2(a), the physical structure is symmetrical. An odd- and even-mode analysis [14] can be adopted to analyze this structure. Based on the mechanism of the resonator resonance, the structure is resonant when its input admittance is zero for both even- and odd-modes, i.e.,

$$Y_{even} = Y_{odd} = 0 \quad (1)$$

The even-mode admittance in Figure 2(b) can be given as

$$Y_e = jY_c \left[\frac{2Y_c \tan(\theta/2) + Y_s \tan \theta_s}{2Y_c - Y_s \tan(\theta/2) \tan \theta_s} \right] \quad (2)$$

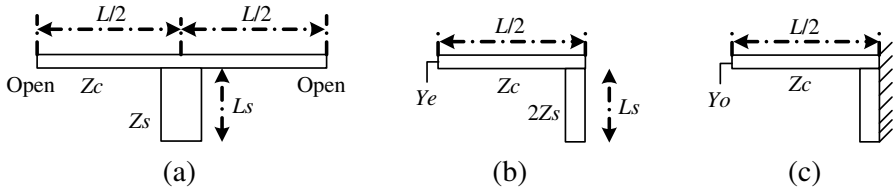


Figure 2. The proposed dual-mode resonator and its even- and odd-mode equivalent circuits. (a) MM resonator. (b) Even-mode. (c) Odd-mode.

where $\theta = \beta L/2$ and $\theta_s = \beta L_s/2$ are the electric length; $\beta = \omega\sqrt{\epsilon_{eff}}/c$ (c is velocity of the light in the free space and ϵ_{eff} denotes the effective dielectric constant of the substrate) is the propagation constant; and $Y_c = 1/Z_c$ is the characteristic admittance of the resonator.

Using Equations (1) and (2), it reads

$$\cot(\theta) \tan(\theta_s) = -2Y_c/Y_s \tag{3}$$

For a special case $Y_s = 2Y_c$, the even-mode resonant frequency can be determined by equation

$$f_e = \frac{cn}{2(L + 2L_s)\sqrt{\epsilon_{eff}}} \quad n = 1, 2, 3, \dots \tag{4}$$

The odd-mode admittance in Figure 2(c) can be expressed as

$$Y_o = 1/(jZ_c \tan \theta) \tag{5}$$

Thus the odd-mode resonant angular frequency can be expressed as

$$f_o = \frac{(2n - 1)c}{2\sqrt{\epsilon_{eff}}L} \tag{6}$$

The resonator topologies in Figure 2 can work as multimode coupled resonators or a dual mode band-pass filter (BPF). The center frequency of the multimode BPF can be approximated by averaging the fundamental even- and odd-mode frequencies as

$$f_0 = \frac{1}{2} (f_e + f_o) = \frac{1}{2} \left[\frac{c}{2L\sqrt{\epsilon_{eff}}} + \frac{c}{2(L + 2L_s)\sqrt{\epsilon_{eff}}} \right] \tag{7}$$

The electric coupling between two modes is characterized by the coupling coefficient K [15] which can be computed from the fundamental even- and odd-mode frequencies as

$$K = \frac{f_o^2 - f_e^2}{f_o^2 + f_e^2} = \frac{(L + 2L_s)^2 - L^2}{(L + 2L_s)^2 + L^2} \tag{8}$$

The fundamental odd-mode resonant frequency is fixed when the length L is fixed, while the fundamental even-mode operating frequency can be adjusted by change the length L_s or width W_s of the perturbation stub. By increasing L_s , the fundamental even-mode resonant frequency can be shifted in a wide range, whereas the fundamental odd-mode resonant frequency is almost preserved. Although the analysis is based on the dual-mode case, as demonstrated in [15], it is possible to generate multimode behaves up to fourth order when the strong I/O couplings is provided and parasitic mode may exist between the strong coupled lines.

3. MULTIMODE BAND PASS FILTER DESIGN

As shown in Figure 2, the stub in the center in the single multimode resonator is used to achieve multimode operation up to four modes under over-exciting in the I/O and one additional zero point simultaneously [15]. The unit multimode resonator MMR1 or MMR2 can be represented by the equivalent circuit network in the previous section. The two cell multimode filter, as the topology given in Figure 3(a), can be represented by two equivalent circuit networks in cascading [18]. The couplings from source to MMR1 and from MMR2 to load are denoted as MS_1 and M_{2L} . The internal coupling between MMR1 and MMR2 is represented by M_{12} . The filter is designed to operate in 6 GHz \sim 8 GHz. As shown in Figure 3(b), the whole filter layout is symmetrical to the reference line “A” and the

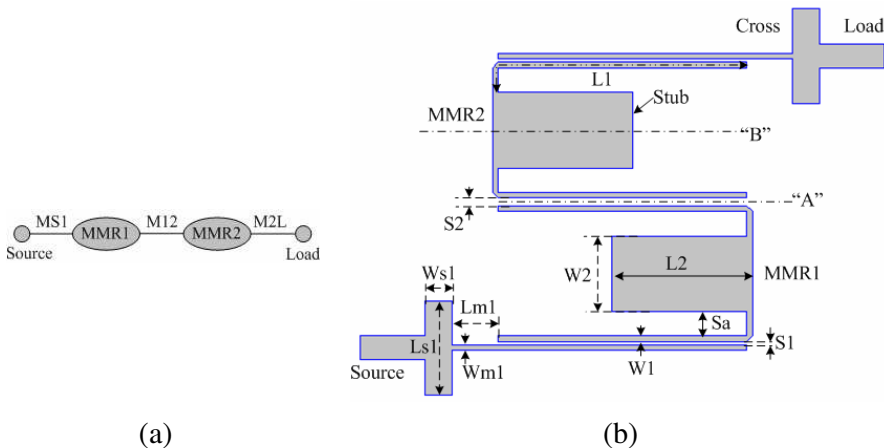


Figure 3. The proposed network model and dual-mode filter. (a) Dual-mode filter topology. (b) Dual-mode filter structure.

multimode resonator MMR1 or MMR2 is symmetrical to the center reference line “B” and the coupling MS1 is designed to be equal to M2L as the symmetrical condition. The coupling gap $S1$ is to control the coupling between the input and the multimode resonator MMR1 and the internal gap $S2$ between multimode resonators is to control the internal coupling between MMR1 and MMR2. For the high-order multimode filter, the inter-stage coupling between the MMR1 and MMR2 actually affects all of the resonant modes in each of the multimode resonators. For this case, there are three degenerate modes from either MMR1 or MMR2 affected. The full-wave simulation and optimization are required to get good response of the multimode filter. The designed dimensions are: $Ls1 = 1.6$ mm, $Sa = 0.76$ mm, $W2 = 2.38$ mm, $L2 = 4.42$ mm, $L1 = 8.6$ mm, $Ws1 = 0.4$ mm, $S1 = 0.11$ mm, $S2 = 0.21$ mm, $Lm1 = 1.45$ mm, $W1 = 0.18$ mm, $Wm1 = 0.15$ mm.

The simulation results are shown in Figure 4. There are totally six resonant modes generated in the pass band of the multimode filter. It can be seen that a very good rolloff is achieved. The additional two resonator modes are generated due to the strong input and output coupling, i.e., over-exciting in source/load (compared to the four modes of the two dual mode resonators) may generate additional mode as presented in [15]. The simulated insertion loss is around $0.7 \sim 1.2$ dB. The deep stopband rejection of more than 50 dB is achieved up to 17.3 GHz. Above 17.3 GHz, there are several parasitic resonant modes at around 18 GHz, 23 GHz and 30 GHz. The relative wide stopband of the proposed multimode BPF is due to the two perturbation stubs which generate additional zeros in the stopband [15]. The layout of the filter excluded the loaded cells LC1 and LC2, is shown in Figure 3(b).

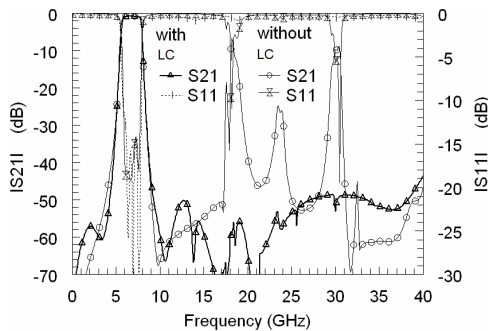


Figure 4. The comparison of the characteristics of the proposed filter with and without loading cells (LC).

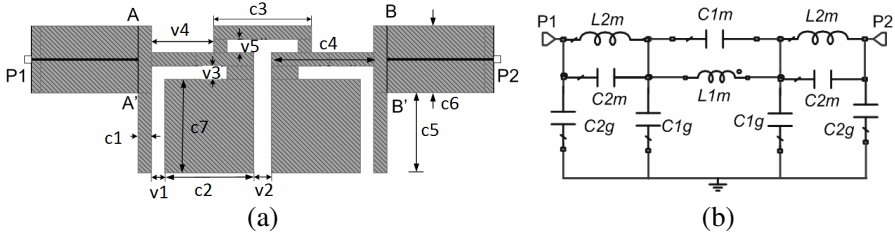


Figure 5. The proposed loading cell structures for stopband extension. (a) Loading cell. (b) Model of the loading cell.

4. STOP BAND EXTENSION BY LOADING CELLS

To further extend the stopband while keeping the size as compact as possible, a loaded cell structure is proposed as shown in Figure 5. The parasitic coupling path from the hairpin [17] are form a source-load coupling path, thus the elliptical response and wide stopband can be achieved simultaneously. The stopband of the loading cell is purposely designed in the far stopband of the multimode BPF, where the parasitic resonant modes of the BPF appear. Since the filter physical size is decreased with the increase of the cutoff frequency, the benefit of this approach is that both wide stopband and compact size can be achieved simultaneously. The loading cell can be represented as the third-order elliptical low pass lumped elements model as shown in Figure 5(b). The dominant low pass cell is the step-impedance resonator hairpin which modelled as the elliptical low pass filter composed by $L1m$, $C1m$ and $C1g$. $C1m$ and $C2m$ denote the parasitic electric coupling path from source to load of the connection nodes. While the inductor with length $c4$ and stub with width of $c1$ can be represented by $L2m$, $C2m$ and $C2g$. By using the loading cell, it is possible to generate more than two zeros in the far stopband. The dimensions of LC1 are $v1 = v2 = v5 = 6$ mil; $v3 = 8$ mil; $v4 = 28$ mil; $c1 = 6$ mil; $c2 = 40$ mil; $c3 = 44$ mil; $c4 = 46$ mil; $c5 = 36$ mil; $c6 = 30$ mil; $c7 = 42$ mil. The dimensions of LC2 are $v1 = v2 = v5 = 6$ mil; $v3 = 8$ mil; $v4 = 14$ mil; $c1 = 6$ mil; $c2 = 40$ mil; $c3 = 72$ mil; $c4 = 46$ mil; $c5 = 36$ mil; $c6 = 30$ mil; $c7 = 50$ mil. LC1 and LC2 are connected through a 50 Ohm line with length of 6 mil. The loading cells (LC) are designed with high cutoff frequencies (13.5 GHz and 20 GHz for LC2 and LC1 respectively) to achieve compact size. The loading cells characteristics are extracted through de-embedding from I/O ports (P1 and P2) to reference plane A-A' and B-B'. The simulated results of LC1 and LC2 are compared in Figure 6. It is found that at least two zeros are generated. The loaded cells behave as a low-pass elliptical filter with

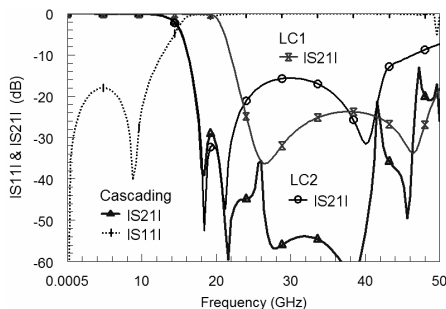


Figure 6. Frequency responses of LC1, LC2 cascading cell of LC1 and LC2.

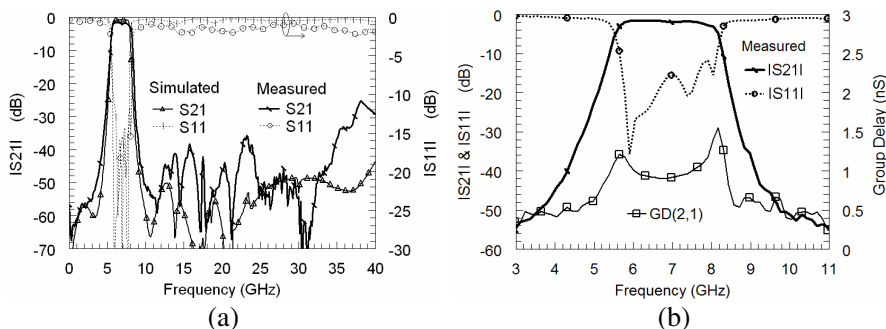


Figure 7. Simulation and measurement results of the proposed filter. (a) Theory and experiment results of the proposed filter. (b) The measured results of narrow band response.

two zeros in the stopband, one in close stopband and the other is in the far stopband. The generation of two or three zeros are due to the cross electric coupling or source to load coupling corresponding to the connection nodes, $Cm1$ and the self-resonance of the resonators. While keeping good matching and low insertion loss below 8 GHz, the designed loading cells LC1 and LC2 are cascaded in each port of the two I/O ports to achieve wider and deeper stopband. The passband and first stopband zero of the cascading loaded cells are almost the same as that of the loaded cell LC2. The simulation results of the multimode BPF with and without loaded cells (LC1 and LC2) are compared in Figure 4. It can be seen that the responses in the passband with and without loaded cells are almost the same. The stopband response of the multimode BPF with loaded cells is dramatically improved with better than 45 dB rejection up to 39 GHz.

5. RESULTS AND DISCUSSIONS

The planar 6 ~ 8 GHz multimode filter with LCs is designed and fabricated using Rogers Ro5880 materials. Multimode filter is measured with HP8722ES vector network analyzer together with 3.5 mm connector calibration kits. The universal substrate test fixtures WK-3001-B from Microwave Inter-continental Inc. are used for I/O port connections for measurement. The simulated results and the measured results are compared in Figure 7(a). The measured 1-dB bandwidth is from 5.7 GHz to 8.0 GHz (the fractional bandwidth is 32.8%) which is a little wider than that of simulated results (6 ~ 8 GHz) using circuit simulator in ADS2005A. Both simulated and measured results of the multimode filter show the return loss of better than 10 dB in passband and good rejection in the stopband. From 9.2 GHz to 22 GHz, the rejection is more than 40 dB. From 9.2 GHz to 37 GHz, which is the fifth harmonic range of the traditional half-wavelength resonator, the rejection is more than 30 dB. The measured minimum insertion loss, including the SMA connector losses of test fixture in I/O ports, is only 1.7 dB. The measurement results of the group delay and the narrow band response for the multimode filter are illustrated in Figure 7(b). The group delay has a variation of 0.9 ~ 1.4 nS in the passband. The photograph of the multimode filter is shown in Figure 8. The effective size of the filter is only 19 mm by 12.7 mm, ($0.61\lambda_g \times 0.41\lambda_g$, where λ_g is the wavelength at center operating frequency on the substrate), which is close to that of the traditional half-wavelength resonator at the center operating frequency.

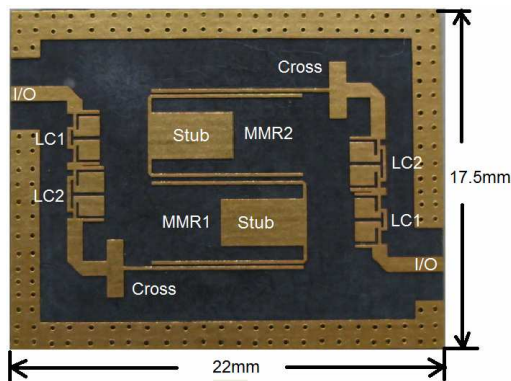


Figure 8. Photograph of the proposed multi-mode filter.

6. CONCLUSION

In this paper, a cascaded multimode filter structure using stub perturbation is introduced and investigated. The stubs are used to achieve multimode operation and additional zero point simultaneously. A compact loading cell with elliptical low-pass response is introduced into the multimode BPF to further extend the stopband of the BPF. The measured results of the proposed filter demonstrates not only low insertion loss and compact size through multimode operation, but also a wide stopband and high stopband rejection through the intrinsic zero point generation, of the open stubs together with the loaded cells with elliptical low-pass response. These characteristics are challenging to be achieved simultaneously using traditional filter configurations.

REFERENCES

1. Chiou, Y.-C. and J.-T. Kuo, "Planar multiband bandpass filter with multimode stepped-impedance resonators," *Progress In Electromagnetics Research*, Vol. 114, 129–144, 2011.
2. Huang, X.-G., Q.-Y. Feng, and Q.-Y. Xiang, "High selectivity broadband bandpass filter using stub-loaded quadruple-mode resonator," *Journal of Electromagnetic Waves and Applications*, Vol. 26, No. 1, 34–43, 2012.
3. Wang, L. and B.-R. Guan, "Compact and high selectivity dual-band bandpass filter using nested dual-mode defected ground structure resonators," *Journal of Electromagnetic Waves and Applications*, Vol. 26, No. 4, 549–559, 2012.
4. Lee, J. R., J. H. Cho, and S. W. Yun, "New compact bandpass filter using microstrip $\lambda/4$ resonators with open stub inverter," *IEEE Microwave and Guided Wave Letters*, Vol. 10, 526–527, Dec. 2000.
5. Mondal, P. and M. K. Mandal, "Design of dual-band bandpass filters using stub-loaded open-loop resonators," *IEEE Trans. Microwave Theory Tech.*, Vol. 56, 150–155, Jan. 2008.
6. Kuo, Y. T., "Analytical design of two-mode dual-band filters using E-shaped resonators," *IEEE Trans. Microwave Theory Tech.*, Vol. 60, 250–260, Feb. 2012.
7. Hong, J.-S. and M. J. Lancaster, *Microstrip Filters for RF/Microwave Applications*, John Wiley & Sons, Inc., 2001.
8. Sagawa, M., K. Takahashi, and M. Makimoto, "Miniaturized hairpin resonator filters and their application to receiver front-

- end MIC's," *IEEE Trans. Microwave Theory Tech.*, Vol. 37, 1991–1996, Dec. 1989.
9. Ma, K., K. S. Yeo, J.-G. Ma, and M. A. Do, "An ultra-compact hairpin band pass filter with additional zero points," *IEEE Microwave and Wireless Components Lett.*, Vol. 17, 262–264, Apr. 2007.
 10. Ma, K., J.-G. Ma, K. S. Yeo, and M. A. Do, "A compact size coupling controllable filter with separated electric and magnetic coupling paths," *IEEE Trans. Microwave Theory Tech.*, Vol. 54, No. 3, 1113–1119, Mar. 2006.
 11. Awai, I., A. C. Kundu, and T. Yamashita, "Equivalent-circuit representation and explanation of attenuation poles of a multimode dielectric-resonator bandpass filter," *IEEE Trans. Microwave Theory Tech.*, Vol. 46, 2159–2163, Dec. 1998.
 12. Zhu, L., P. Wecowski, and K. Wu, "New planar multimode filter using cross-slotted patch resonator for simultaneous size and loss reduction," *IEEE Trans. Microwave Theory and Tech.*, Vol. 47, No. 5, 650–654, May 1999.
 13. Hong, J.-S. and M. J. Lancaster, "Microstrip triangular patch resonator filters," *IEEE MTT-S Int. Symp. Dig.*, 331–334, 2000.
 14. Zhu, L., S. Sun, and W. Menzel, "Ultra-wideband (UWB) bandpass filters using multiple-mode resonator," *IEEE Microwave and Wireless Components Lett.*, Vol. 15, No. 11, 796–798, Nov. 2005.
 15. Ma, K., K. C. B. Leong, R. M. Jayasuriya, and K. S. Yeo, "A wideband and high rejection multimode bandpass filter using stub perturbation," *IEEE Microwave and Wireless Components Lett.*, Vol. 19, 24–26, Jan. 2009.
 16. Shaman, H. and J.-S. Hong, "A novel ultra-wideband (UWB) bandpass filter (BPF) with pairs of transmission zeroes," *IEEE Microwave and Wireless Components Lett.*, Vol. 17, No. 2, 121–123, Feb. 2007.
 17. Hsieh, L.-H. and K. Chang, "Compact elliptic-function low-pass filters using microstrip stepped-impedance hairpin resonators," *IEEE Trans. Microwave Theory and Tech.*, Vol. 51, No. 1, 193–199, Jan. 2003.
 18. Bastioli, S., C. Tomassoni, and R. Sorrentino, "A new class of waveguide dual-mode filters using TM and nonresonating," *IEEE Trans. Microwave Theory and Tech.*, Vol. 58, No. 12, 3909–3917, Dec. 2010.